Time-Domain Modelling of Group-Delay and Amplitude Characteristics in Ultra-Wideband Printed-Circuit Antennas

Hung-Jui Lam, Yinying Lu, Huilian Du, Poman P.M. So and Jens Bornemann

1 Introduction

With the release of the 3.1–10.6 GHz band for ultra-wideband (UWB) operation, a variety of typical UWB applications evolved; examples are indoor/outdoor communication systems, ground-penetrating and vehicular radars, wall and through-wall imaging, medical imaging and surveillance, e.g. [1, 2]. Many future systems will utilize handheld devices for such short-range and high bandwidth applications. Therefore, the realization of UWB antennas in printed-circuit technologies within relatively small substrate areas is of primary importance. And a number of such antennas with either microstrip, e.g. [3, 4, 5, 6, 7, 8, 9, 10] or coplanar waveguide feeds, e.g. [11, 12, 13, 14, 15, 16, 17, 18, 19, 20, 21, 22, 23], and in combined technologies, e.g. [24, 25], have been presented recently, mostly for the 3.1–10.6 GHz band, but also for higher frequency ranges, e.g. [26].

Since UWB systems involve the transmission and reception of short pulses, the variations of radiated amplitudes and phases over frequency contribute to the distortion of the pulse. While the amplitude variation is usually indicated by changes in the peak gain or radiation patterns, the frequency-dependent phase variation is often

Hung-Jui Lam

Department of Electrical and Computer Engineering, University of Victoria, P.O. Box 3055 STN CSC, Victoria, B.C., V8W 3P6, Canada

Yinying Lu

Department of Electrical and Computer Engineering, University of Victoria, P.O. Box 3055 STN CSC, Victoria, B.C., V8W 3P6, Canada

Huilian Du

Department of Electrical and Computer Engineering, University of Victoria, P.O. Box 3055 STN CSC, Victoria, B.C., V8W 3P6, Canada

Poman P.M. So

Department of Electrical and Computer Engineering, University of Victoria, P.O. Box 3055 STN CSC, Victoria, B.C., V8W 3P6, Canada, e-mail: Poman.So@ECE.UVic.CA

Jens Bornemann

Department of Electrical and Computer Engineering, University of Victoria, P.O. Box 3055 STN CSC, Victoria, B.C., V8W 3P6, Canada

omitted, and related data is published only sporadically, e.g., [5, 7, 17, 26]. In order to quantify this behavior, one of two methods is usually applied.

First, in the frequency domain, the spherical wave front in the far field is detected for each frequency, from which the apparent phase center along the antenna surface or axis can be calculated. Alternatively, the phase variation in the near field over the main beam is computed for different phase center points moved from a reference point on the surface of the antenna. Then a valid phase center location is detected if the phase variation over the main beam is within a few degrees. These methods are complicated and time-consuming [26].

Secondly, in the time domain, a transient analysis is performed which leads to the group delay. A pulse, whose frequency spectrum covers the bandwidth of the antenna, is generated, applied at the antenna input and its radiated pulse detected. Both pulses are Fourier transformed and their phase response recorded. The group delay is obtained from the derivative of the phase variation with respect to angular frequency [7].

In this paper, the Transmission-Line Matrix (TLM) method in the time domain is utilized to determine the group delay of two printed circuit UWB antennas. The first one is a recently developed, new coplanar-waveguide antenna [27], the second a published microstrip antenna [9, 10] with so far no information about phase variations.

2 Coplanar UWB Antenna

Figure 1 shows the layout and the superimposed coordinate system of the UWB antenna in coplanar technology. It uses an FR4 substrate of 1mm thickness, an area of $30\,\text{mm} \times 40\,\text{mm}$ (W $\times$ L), a permittivity of $\varepsilon_r = 4.7$ and a loss tangent of
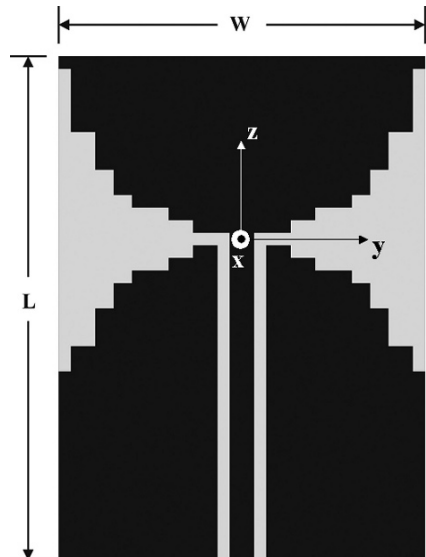

Fig. 1 Layout and coordinate system of UWB antenna in coplanar technology

$\tan \delta = 0.018$. It appears to be a stepped version of a similar antenna presented in [20]. However, there are two fundamental differences. First of all, the antenna in [20] is a slot radiator, which maintains metallic strips at the left and right edges of the substrate. Such metallic strips are missing in Fig. 1 and thus result in a somewhat conical shape of the radiating profile – similar to a tapered slot antenna. Secondly, the stepping is chosen such that the smallest dimension is 0.5 mm. This contributes to low manufacturing sensitivity. However, it also influences the characteristic impedance of the feeding coplanar waveguide, which is significantly higher than the 50 Ω coaxial line to be connected at the input. (Note that the coaxial line is also used to physically connect the two ground planes.) As we will show later, this mismatch is not to the detriment of the antenna performance.

The coplanar UWB antenna was designed using the finite-element software HFSS®. For the evaluation of the group-delay characteristics, the antenna was also analyzed by the TLM time-domain field solver MEFiSTo-3D®. Figure 2 shows a comparison between the input reflection coefficients obtained with both methods. Note that the connection of the input of the antenna to a coaxial cable is included in both methods. Good agreement is observed, thus verifying the antenna's performance at its input terminal. The input return loss as computer by HFSS between 3.1 GHz and 10.6 GHz is better than 9.4 dB.

The peak gain, computed using HFSS at the dots and spline interpolated, is shown in Fig. 3. Its variation versus frequency is comparable to other UWB printed-circuit antennas found in the literature. Note that the direction of the peak gain varies with frequency and, therefore, is not an indication of the amplitude variation in a specific direction.

Such a variation is presented by the normalized radiation pattern. The E-field variation with angle and frequency in the yz-plane (c.f. Fig. 1) is demonstrated in Fig. 4. (For E-plane and H-plane radiation patterns in other planes, the reader is referred to [27].) As we will calculate the amplitude variation using a time-domain technique in the next chapter, it is important to note that in the direction of $\theta = \phi = \pi/2$, the variation versus frequency in Fig. 4 is in the order of 8 to 9 dB.
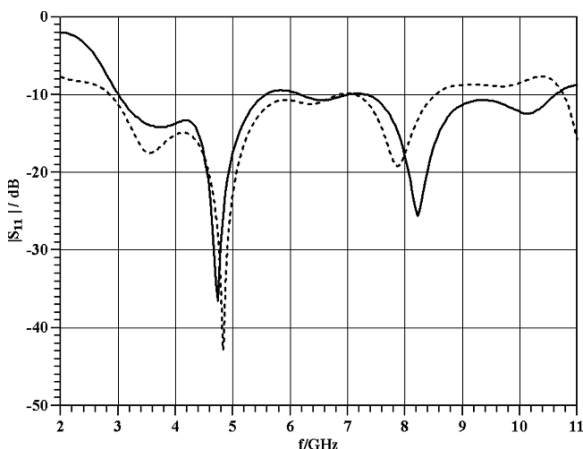

Fig. 2 Comparison of input reflection performance between HFSS (*solid line*) and MEFiSTo-3D (*dashed line*)
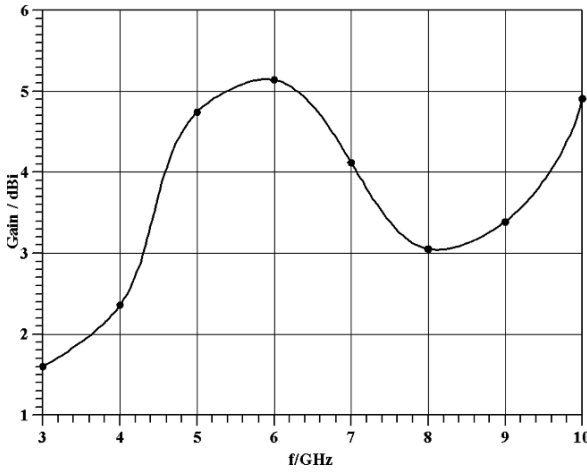
Fig. 3 Peak gain of the UWB antenna in CPW technology computed by HFSS (*dots*) and spline interpolated (*solid line*)
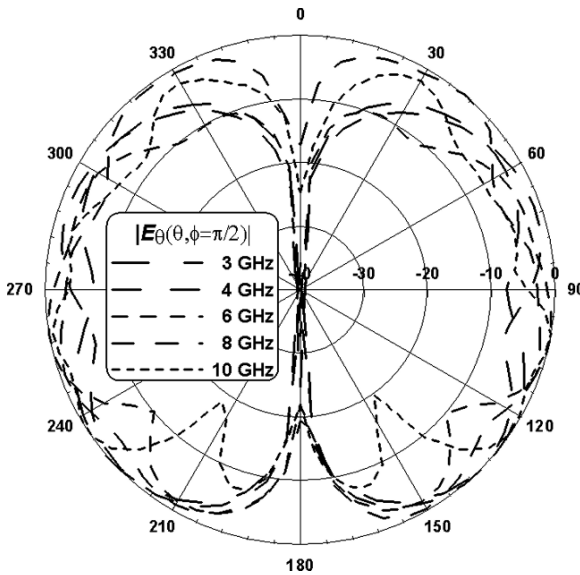

Fig. 4 Normalized E-plane radiation pattern (computed with HFSS) in the yz-plane (c.f. Fig. 1) at various frequencies between 3 GHz and 10 GHz

3 Group Delay and Amplitude Variation

In the first part of this chapter, we will demonstrate the time-domain calculation of the group delay and amplitude variation at the example of the coplanar UWB antenna presented in Chap. 2. The second part applies the same technique to the microstrip antenna presented in [9, 10].

3.1 Coplanar Antenna

Figure 5 shows the setup in MEFiSTo-3D. Since the problem is symmetric with respect to a magnetic wall in the xz-plane (all other walls are absorbing boundaries), only half of the computational space is required. The input of the antenna is excited with a pulse covering the entire frequency spectrum of application. At a point in the far field, probes detect the vertical polarization E_θ and the horizontal polarization E_ϕ. Their orientation with respect to Fig. 1 are depicted in Fig. 6. Note that the coaxial input port and a reference port are included.

Input and detected signals are Fourier transformed to obtain amplitude and phase responses. The group delay is obtained from the derivative of the phase response. Figure 7 shows the input time-domain signal together with its corresponding amplitude (in dB) and phase spectra. Note that the duration of the pulse is about 0.4 ns and the phase variation is in the order of hundreds of degrees.

The radiated signals E_θ (solid lines) and E_ϕ (dashed lines) as detected by the probes in Fig. 5 and their amplitude and phase spectra are shown in Fig. 8. Figure 8a and b confirm that the main polarization is vertical (E_θ) since the detected signal in horizontal polarization (E_ϕ) is at least more than 20 dB below the vertical component. Figure 8c shows the phase variation now in thousands of degrees, which is a result of the ringing of the detected time signal in Fig. 8a. Moreover, notice that the main part of the received pulse in Fig. 8a looks similar to a negative derivative of the input pulse rather than the original input signal in Fig. 7a. Such behaviour is common in antennas that radiate pulses covering a significant frequency spectrum, e.g. [28].

Figure 9a and b show the amplitude and group-delay responses, respectively, of the coplanar UWB antenna fed by a coaxial cable. The amplitude response in the main polarization (solid line) is between −40 and −50 dB which is due to the small
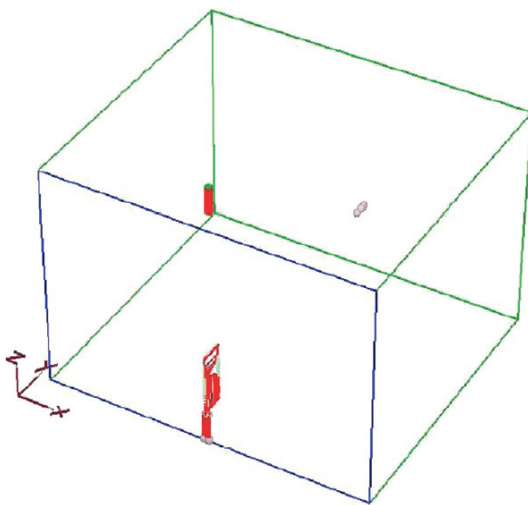

Fig. 5 Setup of one half of the coplanar UWB antenna in MEFiSTo-3D including coaxial input port, probes and coaxial reference port
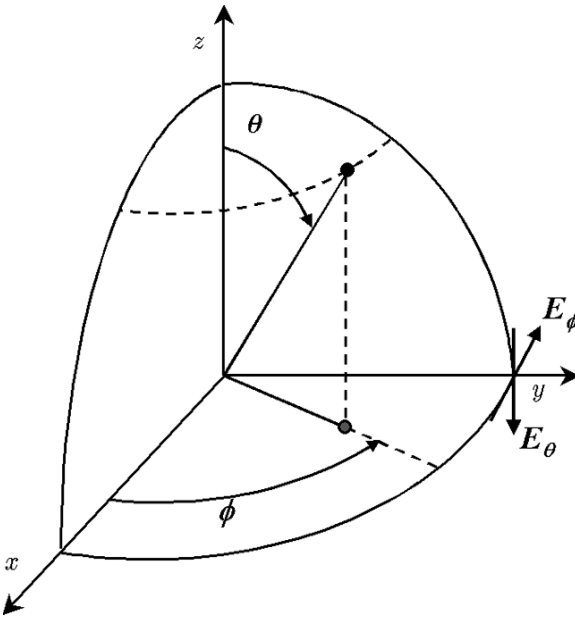
Fig. 6 Orientation of field components received by probes in Fig. 5 with respect to Fig. 1
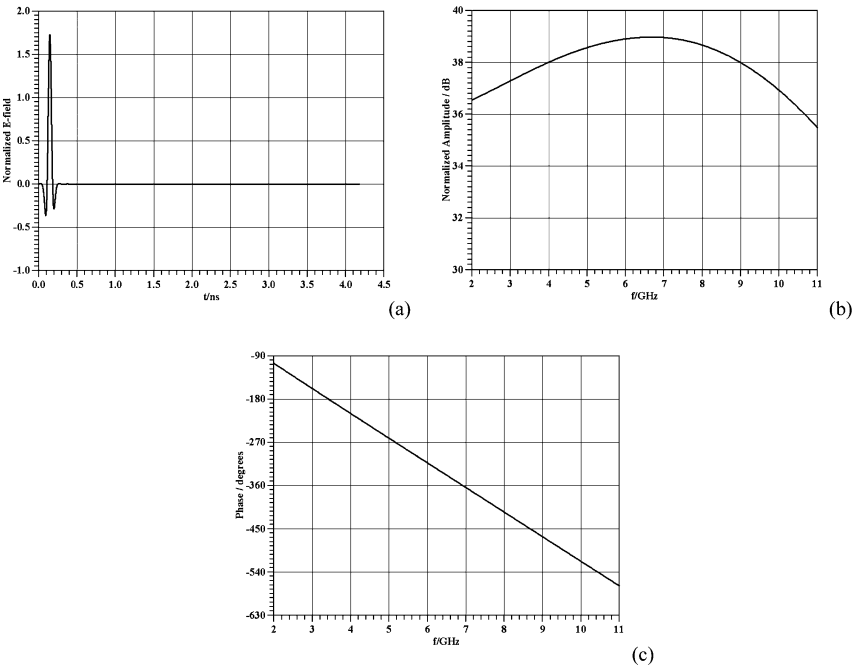

Fig. 7 Time-domain signal (**a**), amplitude spectrum (**b**) and phase spectrum (**c**) at the input of the coaxial cable feeding the coplanar antenna (c.f. Fig. 5)
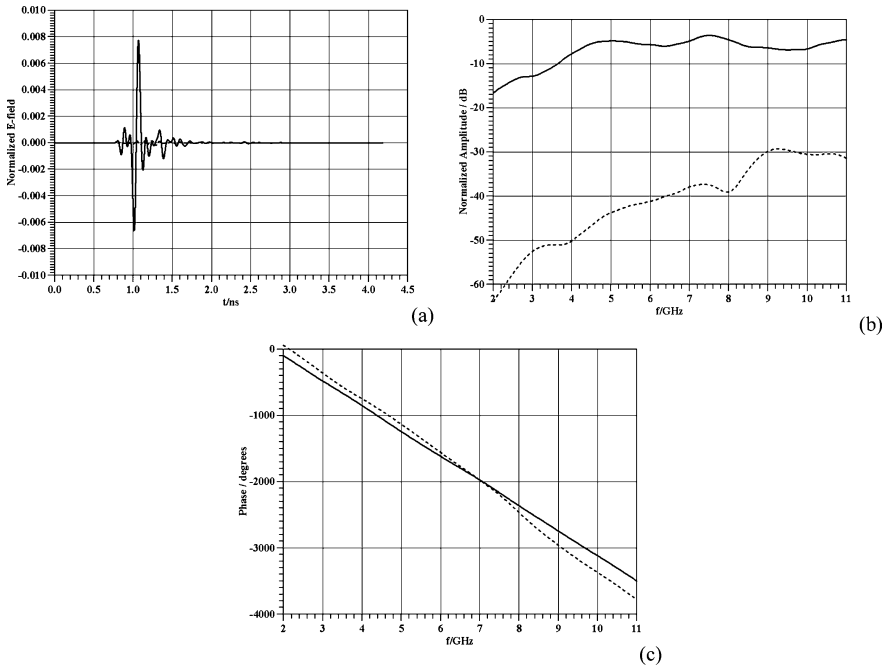
Fig. 8 Radiated time-domain signal (**a**), amplitude spectrum (**b**) and phase spectrum (**c**) detected by the probes; E_θ (*solid lines*) and E_ϕ (*dashed lines*)
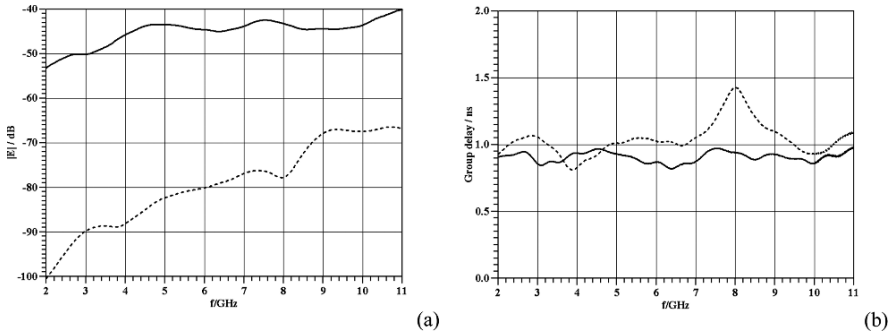

Fig. 9 Amplitude response (**a**) and group-delay characteristic (**b**) of coplanar UWB antenna; vertical polarization E_θ (*solid lines*), and horizontal polarization E_ϕ (*dashed lines*)

effective area of the receiving probes. Since the variations in amplitude and phase (group delay) determine the distortion of the pulse transmitted by the antenna, the respective values – as read from the data plotted in Fig. 9 – are summarized below for both vertical (VP) and horizontal (HP) polarizations.

Frequency range:	3.1 GHz–10.6 GHz
Amplitude variation:	< 8.7 db (VP); < 23 dB (HP)
Group-delay variation:	< 163 ps (VP); < 620 ps (HP)

Note that the amplitude variation of 8.7 dB in vertical polarization (E_θ) is in very good agreement with the radiation patterns displayed in Fig. 4 for individual frequencies between 3 GHz and 10 GHz. Since Fig. 9 was obtained from data computed by the time-domain solver MEFiSTo-3D and Fig. 4 from that of the frequency-domain package HFSS, this agreement (together with Fig. 2) verifies the design and performance of the coplanar UWB antenna.

3.2 Microstrip Antenna

In order to compare the results obtained for the coplanar UWB antenna with those of a different antenna, we apply the above time-domain method to the microstrip UWB antenna presented in [9, 10].

As a verification of the model, Fig. 10 shows the input reflection coefficient (in dB). The VSWR measurements in [9, 10] have been converted to reflection coefficients and are shown as dash-dotted lines. The data from HFSS are shown as dashed lines and are in reasonable agreement with measurements. Note that the HFSS model includes the connection to a coaxial cable. In order to reduce the computational domain, i.e., shorten the long microstrip feed line shown in [9], the coaxial connector could not be modelled in MEFiSTo-3D. Therefore, and especially in the higher frequency range, the agreement between measurements and MEFiSTo-3D is not as good as that with HFSS. However, the basic shape and the reasonably small discrepancies validate the numerical computations.

After exciting the microstrip antenna with a pulse shown in Fig. 7, detecting the radiated signal and calculating amplitude and phase responses, the data presented in Fig. 11 is obtained. Between 3 GHz and 10 GHz, the amplitude variation in vertical polarization is similar to that of the coplanar UWB antenna in Fig. 9a. The signal level difference between horizontal and vertical polarizations in Fig. 11a is smaller than that in Fig. 9a. This is due to the fact that the x-component of the electric field represents the main polarization in a microstrip line if the antenna is oriented in the same way as the coplanar one in Fig. 1.
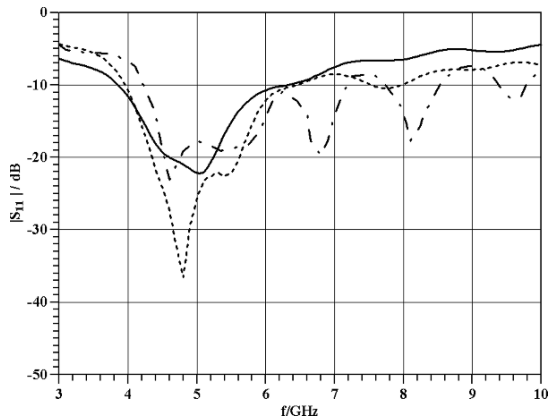

Fig. 10 Input reflection coefficient in dB of the microstrip UWB antenna of [9, 10]; calculated values from VSWR measurements in [9, 10] (*dash-dotted line*), HFSS (*dashed line*) and MEFiSTo-3D (*solid line*)
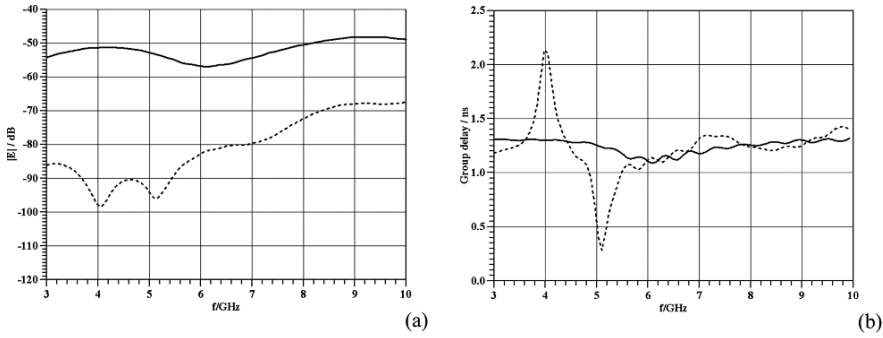
Fig. 11 Amplitude response (**a**) and group-delay characteristic (**b**) of the microstrip UWB antenna in [9, 10]; vertical polarization E_θ (*solid lines*), and horizontal polarization E_ϕ (*dashed lines*)

The group delay performances of the microstrip antenna are inferior to those of the coplanar antenna in both polarizations. The following values are obtained:

Frequency range:	3.0 GHz–10.0 GHz
Amplitude variation:	< 8.8 db (VP); < 31 dB (HP)
Group-delay variation:	< 239 ps (VP); < 1.9 ns (HP)

3.3 Comparison

Both the coplanar and the microstrip antenna display nearly omnidirectional radiation patterns with characteristics slightly distorting towards 10 GHz (c.f. [9, 10] and [27] for details). Over the 3.1–10.6 GHz range, the input reflection coefficient of the coplanar antenna is superior to that of the microstrip antenna. The amplitude variations in vertical polarization are comparable; in horizontal polarization, however, it is 8 dB in favour of the coplanar antenna. The group-delay variations of the coplanar antenna are much smaller than those of the microstrip antenna and, therefore, the coplanar structure of Fig. 1 is better suited for UWB applications.

It is noted that a smaller group-delay variation (< 100 ps) is reported in [7] for a microstrip UWB antenna with two slots in the radiating patch. However, the gain of that antenna is lower that the one reported in Fig. 3 and even drops below 0 dB above 9.8 GHz [7].

4 Conclusion

Time-domain techniques, applied here in form of the TLM solver MEFiSTo-3D, present a viable option for the analysis and modelling of UWB printed-circuit antennas. Amplitude characteristics extracted from the time-domain solution agree well

with frequency-main methods, which are used for the design of UWB antennas. The computation of group-delay data in an actual application of pulsed transmission is one of the clear advantages of time-domain over frequency-domain techniques.

The time-domain modelling procedure presented here is applied to two different printed-circuit UWB antennas, and agreement with frequency-domain computations and measurements is demonstrated.

References

1. L. Yang and G.B. Giannakis, "Ultra-wideband communications: an idea whose time has come", IEEE Signal Proc. Mag., Vol. 21, pp. 26–54, Nov. 2004.
2. International Telecommunication Union, Radiocommunication Study Groups, "Framework for the introduction of devices using ultra-wideband technology", Document 1/85(Rev.1)-E, 09 Nov. 2005.
3. K. Kiminami, A. Hirata and T. Shiozawa, "Double-sided printed bow-tie antenna for UWB communications", IEEE Antennas Wireless Propagat. Lett., Vol. 3, pp. 152–153, 2004.
4. J. Liang, C.C. Chiau, X. Chen and C.G. Parini, "Printed circular disc monopole antenna for ultra-wideband applications", IEE Electronics Lett., Vol. 40, No. 20, pp. 1246–1247, Sep. 2004.
5. S.H. Choi, J.K. Park, S.K. Kim and J.Y. Park, "A new ultra-wideband antenna for UWB applications", Microwave Opt. Technol. Lett., Vol. 40, No. 5, pp. 399–401, Mar. 2004.
6. J. Liang, C.C. Chiau, X. Chen and C.G. Parini, "Study of a printed circular disc monopole antenna for UWB systems", IEEE Trans Antennas Propagat., Vol. 53, pp. 3500–3504, Nov. 2005.
7. Z.N. Low, J.H. Cheong and C.L. Law, "Low-cost PCB antenna for UWB applications", IEEE Antennas Wireless Propagat. Lett., Vol. 4, pp. 237–239, 2005.
8. J. Liang, C.C. Chiau, X. Chen, and C.G. Parini, "Printed circular ring monopole antennas", Microwave Opt. Technol. Lett., Vol. 45, No. 5, pp. 372–375, June 2005.
9. C.-C. Lin, Y.-C. Kan, L.-C. Kuo and H.-R. Chuang, "A planar triangular monopole antenna for UWB communication", IEEE Microwave Wireless Comp. Lett., Vol. 15, pp. 624–626, Oct 2005.
10. H.R Chuang, C.C. Lin and Y.C. Kan, "A printed UWB triangular monopole antenna", Microwave J., Vol. 49, pp. 108–120, Jan. 2006.
11. N. Fortino, G. Kossiavas, J.Y. Dauvignac, and R. Staraj, "Novel antennas for ultrawideband communications", Microwave Opt. Technol. Lett., Vol. 41, No. 3, pp. 166–169, May 2004.
12. W. Wang, S. S. Zhong, and S.-B. Chen, "A novel wideband coplanar-fed monopole antenna", Microwave Opt. Technol. Lett., Vol 43, No. 1, pp. 50–52, Oct. 2004.
13. A.M. Abbosh, M.E. Bialkowski, M.V. Jacob and J. Mazierska, "Investigations into an LTCC based ultra wideband antenna", Proc. Asia-Pacific Microwave Conf., 4p., Suzhou, China, Dec. 2005.
14. C.T.H. Lim, "A GCPW-fed printed antenna for UWB applications", Proc. Asia-Pacific Microwave Conf., 3p., Suzhou, China, Dec. 2005.
15. X. Chen, J. Liang, P. Li, L. Guo, C. C. Chiau and C.G. Parini, "Planar UWB monopole antennas", Proc. Asia-Pacific Microwave Conf., 4p., Suzhou, China, Dec. 2005.
16. H.K. Lee, J.K. Park and J.N. Lee, "Design of a planar half-circle shaped UWB notch antenna", Microwave Opt. Technol. Lett., Vol 47, No. 1, pp. 9–11, Oct. 2005.
17. T.-G.Ma and C.-H. Tseng, "An ultrawideband coplanar waveguide-fed tapered ring slot antenna", IEEE Trans. Antennas Propagat., Vol. 54, pp. 1105–1110, Apr. 2006.

18. Y.-C. Lee, S.-C. Lin and J.-S. Sun, "CPW-fed UWB slot antenna", Proc. Asia-Pacific Microwave Conf., 4p., Yokohama, Japan, Dec. 2006.

19. S. Nikolaou, D.E. Anagnostou, G.E. Ponchak, M.M. Tentzeris and J. Papapolymerou, "Compact Ultra Wide-Band (UWB) CPW-fed elliptical monopole on Liquid Crystal Polymer (LCP)", IEEE AP-S Int. Symp. Dig., pp. 4657–4660, Albuquerque, USA, July 2006.

20. E.S. Angelopoulos, A.Z. Anastopoulos and D.I. Kaklamani, "Ultra-wideband bow-tie slot antenna fed by a cpw-to-cpw transition loaded with inductively coupled slots", Microwave Opt. Technol. Lett., Vol. 48, No. 9, pp. 1816–1820, Sep. 2006.

21. X.-L. Liang, S.-S. Zhong and W. Wang, "UWB printed circular monopole antenna", Microwave Opt. Technol. Lett., Vol. 48, No. 8, pp. 1532–1534, Aug. 2006.

22. J.-S. Sun, Y.-C. Lee and S.-C. Lin, "New design of a CPW-fed ultrawideband slot antenna", Microwave Opt. Technol. Lett., Vol. 49, No. 3, pp. 561–564, Mar. 2007.

23. D.-B. Lin, I.-T. Tang and M.-Y. Tsou, "A compact UWB antenna with CPW-feed", Microwave Opt. Technol. Lett., Vol. 49, No. 3, pp. 564–567, Mar. 2007.

24. Z.N. Chen and X. Qing, "Research and development of planar UWB antennas", Suzhou, China, Dec. 2005.

25. B.L. Ooi, G. Zhao, M.S. Leong, K.M. Chua and C.W.L. Albert, "Wideband LTCC CPW-fed two-layered monopole antenna", IEE Electronics Lett., Vol. 41, No. 16, pp. 9–10, Aug. 2005.

26. K. Rambabu, H.A. Thiart, J. Bornemann and S.Y. Yu, "Ultrawideband printed-circuit antenna", IEEE Trans. Antennas Propagat., Vol. 54, pp. 3908–3911, Dec. 2006.

27. H.-J. Lam and J. Bornemann, "Ultra-wideband printed-circuit antenna in coplanar technology", 2007 IEEE EMC-S Int. Symp. Dig., TU-PM-1-7, 4p, Honolulu, USA, July 2007.

28. D. Ghosh, A. De, M.C. Taylor, T.K. Sarkar, M.C. Wicks and E.L. Mokole, "Transmission and reception by ultra-wideband (UWB) antennas", IEEE Trans. Antennas Propagat. Mag., Vol. 48, pp. 67–99, Oct. 2006.